Binocular Visual Tracking Control Using Feedback Linearization

Bijoy Ghosh[1] and Bhagya Athukorallage[2]

***Abstract*— The binocular eye tracking control problem is considered as a constrained dynamics on a pair of $SO(3)$, the special orthogonal group in three dimensions, from the point of view of a nonlinear multi input multi output (MIMO) system. We consider a pair of eyes and assume that the orientation of every eye satisfies a biologically motivated constraint originally proposed by Listing and Donders. We also assume that the gaze directions of the two eyes pass through a point in the visual space. This would be called coplanarity constraint, essentially because gaze directions of the two eyes would be restricted to lie in a plane. A coupled MIMO dynamical system is thus obtained for the eye-pair simultaneously gazing at a point. The inputs to the MIMO system are the external torque triplet, one for each eye. The output vector contains coordinates of the target direction vectors and includes variables that are to be driven to zero in order to satisfy the Donders' and Co-planarity constraints. The resulting square dynamical system is obtained for the binocular eye-system, leading to an analysis of the feedback linearizing control problem for binocular visual tracking.**

I. INTRODUCTION

We propose to control the pointing directions of a system of two visual sensors (human eyes modeled as a sphere), see Fig. 1, with the goal of tracking a point target moving along a known trajectory in the visual space. Each of the sensors are allowed to rotate, but not translate, controlled by a set of muscle generated torque inputs. The problem of 'pointing control' has previously been studied for a single human eye and human head (see [1] and [2]). The control problem has been addressed using the Lagrangian and Hamiltonian mechanics approach by [3], see [4] for geometry of the eye rotation. In the last two decades, Geometry and control of human eye and head movements have also been introduced in [5], [6], [7], and [8] (see also recent articles by [9], [10]. Most recently, the control problem using 'geometric mechanics' has been extended to the binocular case involving two eyes tracking a point target following an unknown trajectory, see [11]).

The pointing control problem has also been studied using nonlinear systems theory introduced by [12], where after a suitable change of coordinate and feedback, the input output dynamics can be rendered linear and decoupled. For a single eye and head pointing control, this approach has been introduced in [13], [14], [15]. The approach using nonlinear system theory is the subject matter of this paper wherein we describe one simulation result for two eyes tracking a known trajectory in the visual space while maintaining Donders' and coplanarity constraints.

In the last decade, the problem of 'pointing control' has been extended to binocular control; see [16], [17], [18], [19], [20], [21], using geometric mechanics and optimal control and [22], [23], using nonlinear systems theory and feedback linearization. In this paper, our basic approach is to set up the pointing control problem as a MIMO dynamical system (see [13], [14], and [22]), suitably transform the state variables, and choose a state feedback (as proposed by [12]) to render the dynamical system locally linear. It is well known that in order to find such a linearizing feedback, the dynamical system has to have a certain set of relative degrees, which is equivalent to asking that an associated decoupling matrix maintains full rank.

We model visual sensors by a rotating sphere and control one, or, in the binocular case, two such sensors. Assuming that the orientation matrices of the sensors nominally satisfy a constraint originally proposed by Donders (see [24], for the head movement problem) and go by the name Donders' Law. The control objective of this paper is to use linearizing feedback to direct the gaze-pointing vector from a pre-specified initial to a final point while maintaining the **Donders' constraint**. Additionally, the control objective is to ensure that the pointing directions of the sensors are pairwise coplanar (**Co-planarity constraint**), implying that all sensors are simultaneously gazing at some point in $\mathbb{R}^3$. A preliminary discussion on binocular vision has already been introduced in [22].

Results from [13] have shown that for points in a suitably restricted subset $\mathcal{H}_{\bar{\psi}}$ of SO(3), that satisfy the Donders' constraint, one can locally linearize the eye or head rotation dynamics by a static state feedback (i.e. the relative degree constraint is satisfied locally at every point on the Donders' surface). The question, we raised in [22] and [21] is to estimate the size of the local neighborhood $\mathcal{N}$. For monocular sensing, the size of $\mathcal{N}$ is estimated by computing distance between the 'Donders' surface' and a '**Monocular Singularity Surface**', where the associated Decoupling matrix is singular, and consequently loses its relative degree. Earlier, the size of $\mathcal{N}$ estimation was carried out using Novelia and O'Reilly [25], [26] parameterization of $\mathbf{SO(3)}$. This computation was repeated, using the well known Tait-Bryan parameterization (see [8]) in [14]. The binocular sensing problem was introduced in [21], where it was shown that the associated singularity surface factors into three parts. The first two are the monocular singularity surfaces that were present in monocular sensing, one for each sensor. The third part is a '**Mixed Singularity Surface**', that is independent

[1]Bijoy K. Ghosh is with the Department of Mathematics and Statistics, Texas Tech University, Lubbock, TX 79409, USA. bijoy.ghosh@ttu.edu

[2]Bhagya Athukorallage is with Department of Mathematics, Williams College, Williamtown, MA 01267, USA ba9@williams.edu

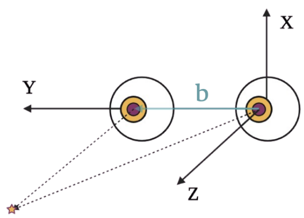

Fig. 1: Binocular sensor array: the centers of the left and the right eyes are located respectively at $(0,0,0)$ and $(0,b,0)$. Note that the center of the axes is assumed to coincide with the left eye, upward-pointing axis is the positive $x-$axis while the forward-pointing axis is the positive $z-$axis. The $y-$axis joins the center of the two eyes and the direction from left to right is chosen positive. Curly arrows (in blue) indicate the positive (clockwise, viewed from the axis center) rotation about each axis. The blue dot is the target, and the two red arrows are the eye-gaze directions.

of the orientations of the sensors, but depend only on the gaze directions.

In this paper, we extend our work in [14], [21], [22] and construct a tracking controller that follows a certain known trajectory while imposing coplanarity and Donders' constraints. The controller is computed using a linearized dynamics, and the control to the nonlinear binocular eye system is recovered.

II. Eye Orientation and the Quaternion Connection

In the following, we sketch some of the main ideas from [13], [21], and [22]. Let R be a point in $\mathbf{SO(3)}$ with column vectors denoted by $R_i, i=1,2,3$. The columns of R can be associated with a frame attached to the visual sensor and would therefore correspond to a specific orientation. Let us denote by $\{r_{ij}\}_{i,j=1,2,3}$ the components of the rotation matrix R. R_3 would be called *gaze pointing direction*. We consider the sensor orientation in the right-handed system, denoted by symbol x-y-z, in $\mathbb{R}^3$, where R_3 corresponds to the z-coordinate, R_1 the x-coordinate and finally R_2 the y-coordinate. As described in [13], the sensor orientation is confined to a subset of $\mathbf{SO(3)}$ given by

$$\mathcal{H} := \{R \in \mathbf{SO(3)} \,|\, \text{trace}(R) > 0 \text{ and } r_{33} > 0\}\,. \tag{1}$$

Associated with a rotation matrix R, there is a unit quaternion $q = [q_0 \quad q_1 \quad q_2 \quad q_3]^T \in \mathbb{S}^3$. This quaternion connection is well known in the literature (see [27]). Let us begin with the space of quaternions denoted by $\mathbf{Q}$, see [28] and write each $q \in \mathbf{Q}$ as $q_0\vec{\mathbf{1}} + q_1\vec{\mathbf{i}} + q_2\vec{\mathbf{j}} + q_3\vec{\mathbf{k}}$. Space of unit quaternions will be identified with the unit sphere $\mathbf{S^3}$, and can be written as

$$q = \cos\left(\frac{\phi}{2}\right)\vec{\mathbf{1}} + \sin\left(\frac{\phi}{2}\right)n_1\vec{\mathbf{i}} + \sin\left(\frac{\phi}{2}\right)n_2\vec{\mathbf{j}} + \sin\left(\frac{\phi}{2}\right)n_3\vec{\mathbf{k}}, \tag{2}$$

where $\phi \in [0, 2\pi]$ is an angle variable and $\vec{n} = \langle n_1, n_2, n_3\rangle$ is a unit axis vector in $\mathbb{R}^3$. We denote by $\mathbf{rot}$, the standard map from $\boldsymbol{S^3}$ into $\mathbf{SO(3)}$ which maps the quaternion q to an orthogonal matrix that rotates a vector in $\mathbb{R}^3$ around the axis of rotation $\vec{n}$ by a counterclockwise angle ϕ (see Fig. 2). It is easy to verify (see (3) in [7]) that

$$\mathbf{rot}(q) = \begin{bmatrix} q_0^2+q_1^2-q_2^2-q_3^2 & 2(q_1q_2-q_0q_3) & 2(q_1q_3+q_0q_2) \\ 2(q_1q_2+q_0q_3) & q_0^2+q_2^2-q_1^2-q_3^2 & 2(q_2q_3-q_0q_1) \\ 2(q_1q_3-q_0q_2) & 2(q_2q_3+q_0q_1) & q_0^2+q_3^2-q_1^2-q_2^2 \end{bmatrix}. \tag{3}$$

The orthogonal matrix (3) can be associated with the orientation of a rotating rigid body as follows: Each column of (3) is a mutually orthogonal unit vector. We can associate the three column vectors to three body coordinates that describe the orientation. The rotating rigid body, viz. the human eye, has a specific 'gaze direction,' a vector whose direction is what we propose to control. We use the convention that the gaze direction is given by the third column of the rotation matrix (3). We therefore have the following projection map, projecting the orientation matrix (3) to a gaze direction vector

$$\mathbf{proj} : \mathbf{SO(3)} \to \mathbf{S^2},$$

where

$$\mathbf{rot(q)} \longmapsto \begin{bmatrix} 2(q_1q_3+q_0q_2) \\ 2(q_2q_3-q_0q_1) \\ q_0^2+q_3^2-q_1^2-q_2^2 \end{bmatrix}. \tag{4}$$

Typically our interest is to control the gaze vector (4) so that it is pointing towards a suitable point target (see Fig. 1). In the literature on binocular eye movement control, a general Donders' constraint is also of interest, see [29] where torsional movements allow fusion of images from the two eyes.

Next we introduce a quadratic Donders' constraint. Donders' constraint in a quadratic polynomial form was originally introduced in [30], [31] and describes a quadratic surface using quaternion parameters q_0, q_1, q_2, q_3. In this paper we consider a simplified form of the quadratic Donders' surface given by

$$q_0\, q_3 = h_D(q_1, q_2), \tag{5}$$

where we define the polynomial h_D as

$$h_D(q_1, q_2) \ := \ c_{11}q_1^2 + c_{12}q_1\, q_2 + c_{22}q_2^2. \tag{6}$$

The simplified Donders' surface (5) contains Listing's plane and the surfaces generated from Fick's and Helmholtz's gimbals, as a special case. Our motivation to consider this simplification is that the relative degree computations in section III-A is well defined entirely over a suitably chosen open set $\mathcal{N}$.

III. Feedback Linearization

A. A Dynamical System for visual sensor array Rotation

We start this section by describing a subset $\mathcal{H}_{\bar{\psi}}$ of $\mathbf{SO(3)}$. Let $\bar{\psi}$ be as described in [13] (Eq. 14, pp. 291), we define

$$\mathcal{H}_{\bar{\psi}} := \left\{R \in \mathcal{H} \,|\, r_{13}^2 + r_{23}^2 < \sin^2\bar{\psi}\right\}.$$

Intuitively, $\mathcal{H}_{\bar{\psi}}$ contains all orientation matrices in $\mathcal{H}$ whose gaze direction vectors are in the allowed region prescribed by Theorem 1 in [13]. We now describe a rotating rigid body dynamics on $\mathcal{H}_{\bar{\psi}}$ and show that such a dynamics is feedback linearizable by a static state feedback in the neighborhood of the Donders' surface. The rigid body dynamics and the output vector are described in the following subsection.

B. A rigid body dynamics with Donders' constraint

Let us consider the following rigid body dynamics [32], [33] of the human head in the 'inertial frame'

$$\dot{R}(t) \;=\; -\,R(t)\hat{\omega}(t), R \in \mathcal{H}_{\bar{\psi}}, \tag{7}$$

$$J\,\dot{\omega}(t) \;= \hat{\omega}\;J\;\omega + T, \tag{8}$$

where $J = \text{diag}\,\{J_1, J_2, J_3\}$ is the moment of inertia matrix, $J_i > 0$, $i = 1, 2, 3$; $T \in \mathbb{R}^3$ are externally applied control torques; and $\omega = [\omega_1, \omega_2, \omega_3]^T \in \mathbb{R}^3$ is the angular velocity vector[1]. We define

$$\hat{\omega} = \begin{bmatrix} 0 & \omega_3 & -\omega_2 \\ -\omega_3 & 0 & \omega_1 \\ \omega_2 & -\omega_1 & 0 \end{bmatrix}. \tag{9}$$

The Donders' constraint (5) can be written as

$$n_3 = \mathcal{D}(n_1, n_2), \tag{10}$$

where n_1, n_2 and n_3 have been defined (see [13]) in terms of r_{ij} and are components of the axis of rotation. An output function

$$\begin{aligned} y &= h(R) = [h_1, h_2, h_3]^T \\ &= [r_{23},\;\; r_{13},\;\; \mathcal{D}(n_1, n_2) - n_3]^T \in \mathbb{R}^3. \end{aligned} \tag{11}$$

is now introduced. Let us now define a proper subset $\mathcal{H}^D_{\bar{\psi}}$ as follows

$$\mathcal{H}^D_{\bar{\psi}} := \left\{ R \in \mathcal{H}_{\bar{\psi}} \,|\, n_3 = \mathcal{D}(n_1, n_2) \right\}. \tag{12}$$

The subset $\mathcal{H}^D_{\bar{\psi}}$ contains all orientation matrices in $\mathcal{H}_{\bar{\psi}}$ that satisfies Donders' constraint (10). For notational convenience, we define $\Xi^D = \mathcal{H}^D_{\bar{\psi}} \times \mathbb{R}^3$, and define $\mathcal{N}$ to be a small enough open neighborhood of Ξ^D inside Ξ.

C. Preliminary remarks from nonlinear MIMO control

We start with a standard definition of a Decoupling matrix.

Definition 3.1 (Vector Relative Degree see [12]): The MIMO system defined by (28a), (28b) has a vector relative degree $[r_1, r_2, r_3]$ at a point $x^\circ \in \mathcal{N}$ if there exists a neighborhood U of x° and there exists a set of positive integers r_1, r_2, r_3 such that, for all $x \in U$, and for all i, j

$$L_{g_i} L_f^{r_j - 2} h_j(x) = 0$$

and the Decoupling matrix

$$N(x) \;:=\; \begin{pmatrix} L_{g_1} L_f^{r_1-1} h_1 & \cdots & L_{g_3} L_f^{r_1-1} h_1 \\ \vdots & \ddots & \vdots \\ L_{g_1} L_f^{r_3-1} h_3 & \cdots & L_{g_3} L_f^{r_3-1} h_3 \end{pmatrix} \in \mathbb{R}^{3\times 3} \tag{13}$$

has full rank.

We note from [13] that the dynamical system (7), (8) and (11) has a vector relative degree $[2, 2, 2]$ at every point on $\mathcal{N}$ and the Decoupling matrix (13) is a 3×3 matrix of rank 3 everywhere on $\mathcal{N}$.

D. Main theorem

Theorem 3.1: ([13]) On a small neighborhood of every point on $\mathcal{N}$, there exist a static feedback law $u^* := a(x) + b(x)v$ such that the rigid body dynamics (7), (8) with output (11) is feedback equivalent to the following controllable linear systems

$$\ddot{z}_i = v_i \text{ for } i = 1, 2, \tag{14}$$

$$\ddot{\xi} = v_3, \tag{15}$$

where $v \in \mathbb{R}^3$ is the new control input vector and new output variables are defined by

$$\begin{bmatrix} z_1 \;\, z_2 \;\, \xi \end{bmatrix}^T := h = \begin{bmatrix} r_{13} \;\, r_{23} \;\, \mathcal{D}(n_1, n_2) - n_3 \end{bmatrix}^T. \tag{16}$$

It is easy to see that $L_{g_i} h_j = 0$ for $i, j = 1, 2, 3$. The Decoupling matrix N in (13) is given by

$$N(x) \;=\; \begin{bmatrix} -r_{22} J_1^{-1} & r_{21} J_2^{-1} & 0 \\ -r_{12} J_1^{-1} & r_{11} J_2^{-1} & 0 \\ L_{g_1} L_f h_3 & L_{g_2} L_f h_3 & L_{g_3} L_f h_3 \end{bmatrix}. \tag{17}$$

We claim [13] that $L_{g_3} L_f h_3(R)|_{\mathcal{H}^D_{\bar{\psi}}} < 0$ so that $\det N(x) \neq 0$ on $\mathcal{H}^D_{\bar{\psi}}$. It follows that the output h has uniformly, the relative degree $[2, 2, 2]$ on $\mathcal{H}^D_{\bar{\psi}}$ and we would have the following local diffeomorphism and feedback law

$$[\, z_1,\;\; z_2,\;\; z_3,\;\; z_4,\;\; \xi_1,\;\; \xi_2 \,] = \; [h_1, h_2, L_f h_1, L_f h_2, h_3, L_f h_3] \tag{18}$$

where $z_3 = \dot{z_1}, z_4 = \dot{z_2}$, and $\xi_2 = \dot{\xi_1}$,[2] and

$$a(x) \;:=\; N^{-1}(x) \left[L_f^2 h_1,\; L_f^2 h_2,\; L_f^2 h_3 \right]^T \text{ and} \tag{19}$$

$$b(x) \;:=\; N^{-1}(x). \tag{20}$$

(see statement of Theorem 3.1). This would render the rigid body dynamics in (7), (8) locally feedback equivalent to the linear system in (14), (15), on Ξ^D.

The linearization method adopted in this paper from [13] has been proposed in [34], [35] in order to decompose the system dynamics into a tangential part and a part transverse to the Donders' submanifold (5).

IV. Binocular Sensor System

As was originally introduced in [21], we consider a pair of rigid spheres that model the binocular sensors. We assume that the frames attached to the two sensors are aligned precisely as described in Section II. The vector separating the centers of the two sensors, lie on the xy-plane and make an angle β with respect to the y-axis. The separating vector is given by $\langle \sin\beta,\, \cos\beta,\, 0\rangle^T$. The equation of motion for each of the two sensors are written in the inertial coordinate as was done in (7), (8). For $i = 1, 2$ we write

$$\dot{R}^i(t) \;=\; -\,R^i(t)\hat{\omega}^i(t), R^i \in \mathcal{H}_{\bar{\psi}}, \tag{21}$$

$$J^i\,\dot{\omega}^i(t) \;= \hat{\omega}^i\;J^i\;\omega^i + u^i \tag{22}$$

[1] The underlying state space of the dynamical system (7), (8) is $\Xi = \mathcal{H}_{\bar{\psi}} \times \mathbb{R}^3$, a 6 dimensional manifold.

[2] Note that $\xi_1 = \xi$, as in (16).

where $J^i = \operatorname{diag}\{J_1^i, J_2^i, J_3^i\}$ is the moment of inertia matrix, $J_j^i > 0$, $j = 1,2,3$; $u^i \in \mathbb{R}^3$ are externally applied control torques; and $\omega^i = [\omega_1^i, \omega_2^i, \omega_3^i]^T \in \mathbb{R}^3$ is the angular velocity vector[3]. We define

$$\hat{\omega}^i = \begin{bmatrix} 0 & \omega_3^i & -\omega_2^i \\ -\omega_3^i & 0 & \omega_1^i \\ \omega_2^i & -\omega_1^i & 0 \end{bmatrix},$$

as in (7) and consider the output function

$$y = [r_{13}^1, r_{23}^1, \mathcal{D}(n_2^1, n_1^1) - n_3^1, r_{13}^2, \Delta_{12}, \mathcal{D}(n_2^2, n_1^2) - n_3^2]^T \in \mathbb{R}^6 \tag{23}$$

where $\Delta_{12} = r_{33}^1 r_{13}^2 - r_{33}^2 r_{13}^1$ when $\beta = 0$. Note in general, that the constraint $\Delta_{12} = 0$ imposes the restriction that the third columns of the rotation matrices are coplanar with respect to the fixed vector $\langle \sin\beta, \cos\beta, 0\rangle^T$. Writing the dynamical system of the 'Binocular System' as a 6−input 6−output system defined on $\mathcal{N} \times \mathcal{N}$, the decoupling matrix takes the form

$$N_{Bino}(x) = \begin{bmatrix} P_{11} & 0 \\ P_{21} & P_{22} \end{bmatrix}, \tag{24}$$

where each P_{ij} matrix has the dimension 3×3, and are described as follows (ignoring the moment of inertia terms)

$$P_{11} = \begin{bmatrix} -r_{22}^1 & r_{21}^1 & 0 \\ -r_{12}^1 & r_{11}^1 & 0 \\ L_{g_1^1} L_f h_3^1 & L_{g_2^1} L_f h_3^1 & L_{g_3^1} L_f h_3^1 \end{bmatrix}, \tag{25}$$

$$P_{21} = \begin{bmatrix} 0 & 0 & 0 \\ \zeta_5 \cos\beta + \zeta_6 \sin\beta & \zeta_7 \cos\beta + \zeta_8 \sin\beta & 0 \\ 0 & 0 & 0 \end{bmatrix}, \tag{26}$$

$$P_{22} = \begin{bmatrix} -r_{22}^2 & r_{21}^2 & 0 \\ \zeta_1 \cos\beta + \zeta_2 \sin\beta & \zeta_3 \cos\beta + \zeta_4 \sin\beta & 0 \\ L_{g_1^2} L_f h_3^2 & L_{g_2^2} L_f h_3^2 & L_{g_3^2} L_f h_3^2 \end{bmatrix}, \tag{27}$$

where

$$\begin{aligned}
\zeta_1 &= r_{13}^1 r_{32}^2 - r_{12}^2 r_{33}^1, \quad \zeta_2 = r_{22}^2 r_{33}^1 - r_{23}^1 r_{32}^2, \\
\zeta_3 &= r_{33}^1 r_{11}^2 - r_{31}^2 r_{13}^1, \quad \zeta_4 = r_{31}^2 r_{23}^1 - r_{21}^2 r_{33}^1, \\
\zeta_5 &= r_{12}^1 r_{33}^2 - r_{13}^2 r_{32}^1, \quad \zeta_6 = r_{32}^1 r_{23}^2 - r_{22}^1 r_{33}^2, \\
\zeta_7 &= r_{31}^1 r_{13}^2 - r_{11}^1 r_{33}^2, \quad \zeta_8 = r_{33}^2 r_{21}^1 - r_{31}^1 r_{23}^2.
\end{aligned}$$

In the binocular system, the feedback law, $u^* = a(x) + b(x)v$, is given by $a(x) := N_{Bino}^{-1}(x)[L_f^2 h_1, L_f^2 h_2, L_f^2 h_3, L_f^2 h_4, L_f^2 h_5, L_f^2 h_6]^T$ and $b(x) := N_{Bino}^{-1}(x)$. Further, the dynamical system (21) and (22) can be written as a control-affine nonlinear 6-input 6-output system defined on $\mathcal{N}$ as follows

$$\dot{x} = f(x) + \sum_{i=1}^{6} g_i(x) u_i, \tag{28a}$$

$$y_i = h_i(x), \; i = 1, \ldots, 6, \tag{28b}$$

[3]For each i, the underlying state space of the dynamical system (21), (22) is $\Xi = \mathcal{H}_{\bar{\psi}} \times \mathbb{R}^3$, a 6 dimensional manifold.

where f and g are smooth vector fields $\mathcal{N} \to \mathbb{R}^{12}$, and all h_i are smooth scalar functions $\mathcal{N} \to \mathbb{R}$. Moreover, from the local feedback linearization theorem the dynamical system (21) and (22) with output given in (23), one gets the controllable linear systems with the new control input vector $v \in \mathbb{R}^6$:

$$\begin{aligned}
\ddot{z}_i(t) &= v_i \quad \text{for } i = 1,2,3 \\
\ddot{\zeta}_i(t) &= v_j \quad \text{for } j = 4,5,6,
\end{aligned} \tag{29}$$

where $[z_1, z_2, \zeta_1, z_3, \zeta_2, \zeta_3]^T = [r_{13}^1, r_{23}^1, \mathcal{D}(n_2^1, n_1^1) - n_3^1, r_{13}^2, \Delta_{12}, \mathcal{D}(n_2^2, n_1^2) - n_3^2]^T$. We consider a reference signal tracking control law that follow the trajectory $\vec{\eta}(t)$ in $\mathbb{R}^3$.

Remark 1: The components of the output vector that follow $\vec{\eta}(t)$ are r_{13}^1, r_{23}^1, and r_{13}^2. Note that the remaining components of the gaze vectors, namely, r_{33}^1, r_{23}^2, and r_{33}^2 are embedded in the Donders' and coplanarity constraints.

The construction of the control signal as follows:

$$\begin{aligned}
v_1(t) &= \ddot{\eta}_1(t) - k_{10}(z_1(t) - \eta_1(t)) - k_{11}(\dot{z}_1(t) - \dot{\eta}_1(t))) \\
v_2(t) &= \ddot{\eta}_2(t) - k_{20}(z_2(t) - \eta_2(t)) - k_{21}(\dot{z}_2(t) - \dot{\eta}_2(t))) \\
v_3(t) &= \ddot{\eta}_3(t) - k_{30}(z_3(t) - \eta_3(t)) - k_{31}(\dot{z}_3(t) - \dot{\eta}_3(t))) \\
v_4(t) &= -k_{40}\zeta_1(t) - k_{41}\dot{\zeta}_1(t) \\
v_5(t) &= -k_{50}\zeta_2(t) - k_{51}\dot{\zeta}_2(t) \\
v_6(t) &= -k_{60}\zeta_3(t) - k_{61}\dot{\zeta}_3(t),
\end{aligned} \tag{30}$$

where each component in $\{\eta_1(t), \eta_2(t), \eta_3(t))\}$ is a twice continuously differentiable functions in $\mathbb{R}^3$. The variables $\zeta_1(t)$ and $\zeta_3(t)$ corresponds to the Donder's constraint of binocular sensors, and lastly, $\zeta_2(t)$ uses to impose the coplanarity constraint. The control gains k_{ij} are selected so that the origin of the linearized system (29) and (30) is asymptotically stable. We next perform a simulation on our reference signal tracking controller, which has not been reported in the literature before.

V. Tracking Control Simulation Results

In this simulation, we consider a pair of visual sensors that individually satisfy Listing's constraint that can be obtained by setting $c_{11} = c_{12} = c_{22} = 0$ in (6). To overcome a numerical difficulty, we express the rotation matrix (3) in terms of the axis-angle parametrization as described in [7]. Further, in order to impose Listing's constraint, $q_3 = 0$, we set $\alpha = 0$, constraining the axis of rotation to lie on the plane $z = 0$. Note that with this new parameterization, the state vector x in (28a) abstractly denotes the state variable $(\phi^1, \alpha^1, \theta^1, \omega_1^1, \omega_2^1, \omega_3^1, \phi^2, \alpha^2, \theta^2, \omega_1^2, \omega_2^2, \omega_3^2)$ of the dynamical system. The gaze vectors of the two sensors (refer to Fig. 1), is assumed to converge at a point that follow the path $(\rho\cos(\omega t), \rho\sin(\omega t), z_0)$ in the visual space.

For the dynamical system described by (29) and the new tracking control (30) are solved using the ODE solver *ODE23t*. The fixed parameters ρ, ω, and z_0 are 1, 0.2π, and 3, respectively. The initial values for the angle parameters are calculated so that a target point lies in the trajectory $(\rho\cos(\omega t), \rho\sin(\omega t), z_0)$ and the gaze vectors of the two

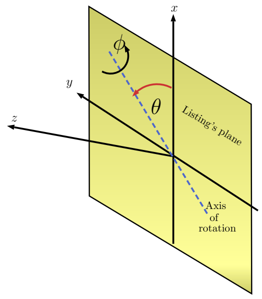

Fig. 2: Axis-angle parametrization under Listing's constraint $q_3 = 0$ as in [10]. The Listing's plane is described by $z = 0$. Angle θ is the angle subtended between the positive axis of rotation on the Listing's plane and the positive x-axis. Angle ϕ is the anticlockwise rotation about the positive axis of rotation.

visual sensors satisfy the co-planarity condition with the initial target point. The parameters selected for the control gains are $k_{i0} = 100$ and $k_{i1} = 20$, $i = 1, 2, \cdots, 6$. We also assume that the moment of inertia matrix for both sensors is equal to I_3.

The simulation results given in Figs. 3 - 4 correspond to the time interval $[0, 2]$. Fig. 3 shows the behavior of the states ϕ, θ, α and angular velocities for both visual sensors. A comparison of the reference signals tracking by output components r^1_{13}, r^1_{23}, and r^2_{13} are given in Fig. 4 (Left). The remaining three output components, which correspond to Co-planarity and Listing's constraints, are plotted in Figs. 4 (Center and Right). It is interesting to note that one would like to satisfy $\alpha = 0$ over the entire time interval as both sensors should satisfy the Listing's constraint, all the time. However, our simulation results show that the angle α of Sensor 2 initially deviates from zero (see Fig. 3), and hence, leaves the Listing's plane (see Fig. 4 (Right)). As a result the corresponding tracking control signal for Sensor 2, $v_6(t)$, asymptotically forces to track the reference signal $y = 0$ indicating that Listing's constraint has been eventually imposed. In addition, initially we see a large angular velocity value about the $x-$axis (ω_1) for both the sensors. Further, Figs. 4 (Center and Right) display that the Coplanarity (Δ_{12}) and Lisiting's constraints approach the target lines $y = 0$ asymptotically.

VI. Conclusion

In the last two decades, two essentially independent control strategies have been introduced to control a binary visual system, with the task of targeting a moving point object. The first one initiated by [5], [6] uses geometric mechanics and culminated in tracking known trajectories see [36] (see [11] for recent results on tracking unknown trajectories). The second strategy, that of exact feedback linearization [12] was initiated by [13] and subsequently resulted in papers such as [21] and [22]. In the last two papers, the structure of the 'singularity surfaces' resulting from the associated decoupling matrix have been discussed. This paper extends the feedback linearization strategy to the problem of tracking a known trajectory, while also maintaining asymptotically, the physiological constraints arising in human eye dynamics, viz. Donders' and Coplanarity.

The extension of the feedback linearization approach to binocular eye tracking of an unknown trajectory will be considered in future research.

References

[1] D. Robinson, "The mechanics of human saccadic eye movement," *The Journal of physiology*, vol. 174, no. 2, pp. 245–264, 1964.

[2] G. C. Peng, T. C. Hain, and B. W. Peterson, "Predicting vestibular, proprioceptive, and biomechanical control strategies in normal and pathological head movements," *Biomedical Engineering, IEEE Transactions on*, vol. 46, no. 11, pp. 1269–1280, 1999.

[3] R. M. Murray, "Nonlinear control of mechanical systems: A lagrangian perspective," *Annu. Rev. Control*, vol. 21, pp. 31–45, 1997.

[4] A. A. Handzel and T. Flash, "The geometry of eye rotations and Listing's law," *Advances in Neural Information Pocessing Systems, (eds) D. S. Touretzky, M.C. Mozer, M. E. Hasselmo*, vol. 8, pp. 117–123, 1966.

[5] A. D. Polpitiya, W. P. Dayawansa, C. F. Martin, and B. K. Ghosh, "Geometry and control of human eye movements," *Automatic Control, IEEE Transactions on*, vol. 52, no. 2, pp. 170–180, 2007.

[6] B. K. Ghosh and I. B. Wijayasinghe, "Dynamics of human head and eye rotations under Donders' constraint," *Automatic Control, IEEE Transactions on*, vol. 57, no. 10, pp. 2478–2489, 2012.

[7] B. K. Ghosh, I. Wijayasinghe, and S. D. Kahagalage, "A geometric approach to head/eye control," *IEEE Access*, vol. 2, pp. 316–332, 2014.

[8] I. Wijayasinghe, J. Ruths, U. Büttner, B. K. Ghosh, S. Glasauer, O. Kremmyda, and J.-S. Li, "Potential and optimal control of human head movement using Tait-Bryan parametrization," *Automatica*, vol. 50 (2), pp. 519–529, 2014.

[9] B. K. Ghosh and B. Athukorallage, "Minimum energy optimal external torque control of human binocular vision," *Control Theory and Technology*, vol. 18, pp. 431–458, 2020.

[10] ——, "Riemannian geometric approach to optimal binocular rotation, pyramid based interpolation and bio-mimetic pan-tilt movement," *Autonomous Intelligent Systems*, vol. 1, no. 3, pp. 1–19, 2021.

[11] A. Bagga, M. Finlay, L. Platonov, B. Tobin, B. K. Ghosh, and B. Athukorallage, "A model predictive control approach to optimal point tracking of unknown trajectories for human binocular eye rotation," *Proc of 2026 American control conference, May 26 - 29, New Orleans, Louisiana, USA*, 2026.

[12] A. Isidori, *Nonlinear Control Systems, 3^{rd} edition*. Springer, 1995.

[13] T. Oki and B. K. Ghosh, "A transverse local feedback linearization approach to human head movement control," *Control Theory and Technology*, vol. 15, no. 4, pp. 245–257, 2017.

[14] B. Athukorallage and B. K. Ghosh, "Feedback linearization of the human head rotation dynamics using Tait-Bryan parameterization," in *Proc. of the 14th IEEE International Conference on Control and Automation, June 12-15, Anchorage, Alaska, USA. (IEEE ICCA 2018)*, 2018, pp. 447–452.

[15] ——, "Eye and head rotation control via feedback linearization," in *Proc. of the 2022 8th International Conference on Control, Decision and Information Technologies, CODIT'22, May 17-20, Istanbul, Turkey.*, 2022, pp. 1501–1505.

[16] I. Wijayasinghe and B. K. Ghosh, "Binocular eye tracking control satisfying hering's law," *Proceedings of the 52^{nd} IEEE Conference on Decision and Control*, pp. 6475–6480, 2013.

[17] M. M. Rajamuni, E. Aulisa, and B. K. Ghosh, "Optimal control problems in binocular vision," *Proceedings of the 19^{th} World Congress of IFAC*, pp. 5283–5289, 2014.

[18] T. Oki and B. K. Ghosh, "Stabilization and trajectory tracking of version and vergence eye movements in human binocular control," *Proceedings of the 2015 European Control Conference (ECC)*, pp. 1573–1580, 2015.

[19] J. Ruths, S. Ghosh, and B. K. Ghosh, "Optimal tracking of version and vergence eye movements in human binocular control," *Proceedings of the 2016 European Control Conference (ECC)*, pp. 2410–2415, 2016.

[20] J. Ruths and B. K. Ghosh, "Helmholtzian strategy to stay in focus with binocular vision," *Proceedings of the 17^{th} European Control Conference*, pp. 2380–2386, 2018.

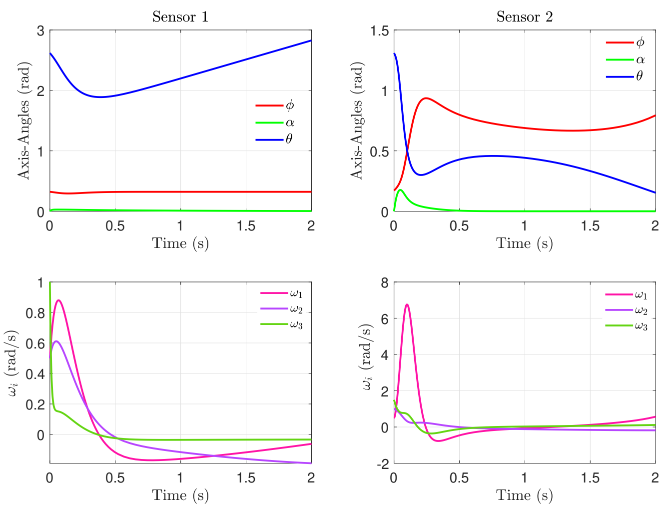

Fig. 3: Variation of the states: axis-angles and angular velocities. The initial values for the angle parameters are calculated so that a target point lies in the trajectory $\left(\cos\frac{\pi}{6}t, \sin\frac{\pi}{6}t, 3\right)$. The initial angular velocities of Sensors 1 and 2 are $\langle 0.5, 0.5, 1.0\rangle$ and $\langle 0.5, 1.0, 1.5\rangle$, respectively.

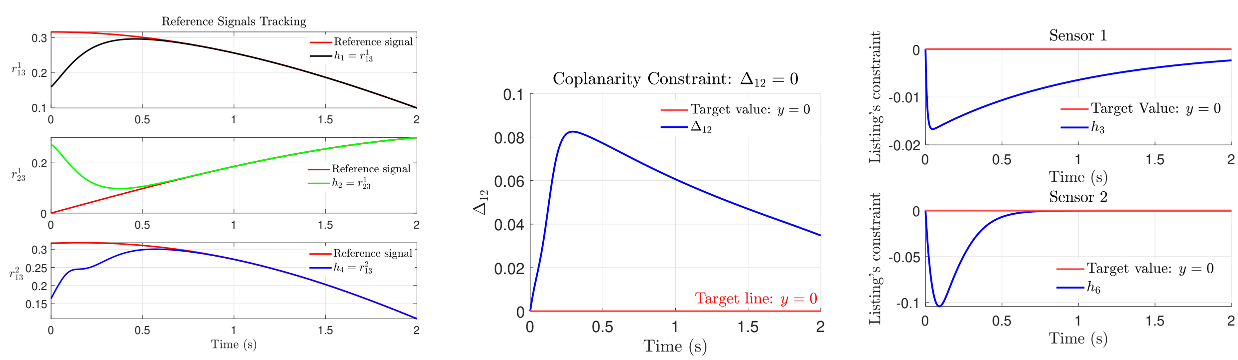

Fig. 4: (Left) Reference signals tracking by the three output components: r^1_{13}, r^1_{23}, r^2_{13}. (Center) Variation of the output vector (h_5) that correspond to the Co-planarity constraint. (Right) Behavior of the output vectors h_3 and h_6 that correspond to the Listing's constraint.

[21] B. K. Ghosh and B. Athukorallage, "Semiglobal feedback linearization of the human head and binocular eye tracking dynamics satisfying Donder's law," in *17th Annual European Control Conference (ECC), June 15th, Limassol, Cyprus.*, 2018, pp. 2684–2690.

[22] B. Athukorallage and B. K. Ghosh, "Human head and binocular eye movement control via feedback linearization," in *Proc. of the 2018 American Control Conference (ACC), June 27-29, Milwaukee, Wisconsin, USA.*, 2018, pp. 6709–6714.

[23] B. K. Ghosh and B. Athukorallage, "Feedback linearization of the rotational dynamics of a flock of target tracking visual sensor array using Tait-Bryan parameterization," in *CPHS Proceedings*, vol. 51, no. 34, 2019, pp. 258–263.

[24] W. Medendorp, J. Van Gisbergen, M. Horstink, and C. Gielen, "Donders' law in torticollis," *Journal of neurophysiology*, vol. 82, no. 5, pp. 2833–2838, 1999.

[25] A. Novelia and O. M. O'Reilly, "On geodesics of the rotation group SO(3)," *Regular and Chaotic Dynamics*, vol. 20, no. 6, pp. 729–738, 2015.

[26] ——, "On the dynamics of the eye: geodesics on a configuration manifold, motions of the gaze direction and helmholtz's theorem," *Nonlinear Dynamics*, vol. 80, no. 3, pp. 1303–1327, 2015.

[27] A. J. Hanson, *Visualizing Quaternions*. Morgan Kaufmann, 2006.

[28] J. Kuipers, *Quaternions and rotation sequences*. Princeton, NJ: Princeton University Press, 1998.

[29] B. J. M. Hess, "On the role of ocular torsion in binocular visual matching," *Scientific Reports*, vol. 8(1):10666, 2018.

[30] O. Kremmyda, S. Glasauer, L. Guerrasio, and U. Büttner, "Effects of unilateral midbrain lesions on gaze (eye and head) movements," *Ann. N. Y. Acad. Sci.*, vol. 1233, pp. 71–77, 2011.

[31] S. Glasauer, M. Hoshi, U. Kempermann, T. Eggert, and U. Büttner, "Three dimensional eye position and slow phase velocity in humans with downbeat nystagmus," *J. Neurophysiol.*, vol. 89, pp. 338–354, 2003.

[32] O. M. O'Reilly, *Intermediate dynamics for engineers*. Cambridge University Press, New York, NY, 2008.

[33] N. A. Chaturvedi, A. K. Sanyal, and N. H. McClamroch, "Rigid-body attitude control," *Control Systems, IEEE*, vol. 31, no. 3, pp. 30–51, 2011.

[34] C. Nielsen and M. Maggiore, "On local transverse feedback linearization," *SIAM Journal on Control and Optimization*, vol. 47, no. 5, pp. 2227–2250, 2008.

[35] C. Nielsen, C. Fulford, and M. Maggiore, "Path following using transverse feedback linearization: Application to a maglev positioning system," *Automatica*, vol. 46, no. 3, pp. 585–590, 2010.

[36] I. B. Wijayasinghe, E. Aulisa, U. B$\ddot{u}$ttner, B. K. Ghosh, S. Glasauer, and O. Kremmyda, "Potential and optimal target fixating control of the human head/eye complex," *Control Systems Technology, IEEE Transactions on*, vol. 23, no. 2, pp. 796–804, 2015.